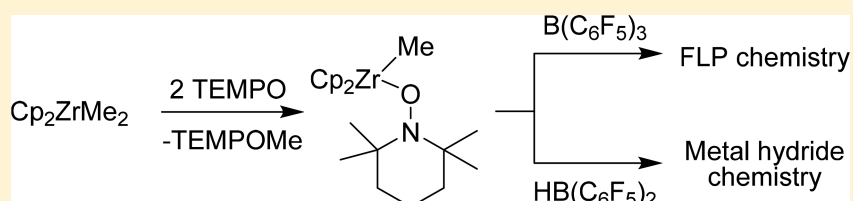


Utilizing the TEMPO Radical in Zirconocene Cation and Hydrido Zirconocene Chemistry

Yun-Lin Liu, Gerald Kehr,^{1b} Constantin G. Daniliuc, and Gerhard Erker^{*1b}

Organisch-Chemisches Institut, Universität Münster, Corrensstraße 40, 48149 Münster, Germany

S Supporting Information



ABSTRACT: Dimethylzirconocene reacts with 2 molar equiv of the persistent radical TEMPO to give the $\text{Cp}_2\text{Zr}(\text{Me})\text{OTMP}$ complex **12** with formation of TEMPOMe. Methyl anion abstraction from **12** with $\text{B}(\text{C}_6\text{F}_5)_3$ generates the $[\text{Cp}_2\text{ZrOTMP}^+]$ cation **13** (with the $[\text{MeB}(\text{C}_6\text{F}_5)_3]^-$ anion) that undergoes a typical intramolecular frustrated Zr^+/N Lewis pair (FLP) reaction with phenylacetylene. With P^tBu_3 it reacts as an intermolecular Zr^+/P FLP trapping carbon dioxide. Complex **12** reacts with $\text{HB}(\text{C}_6\text{F}_5)_2$ also by methyl anion abstraction to form the $\mu\text{-H}$ bridged tight ion pair $\text{Cp}_2\text{ZrOTMP}(\mu\text{-H})\text{BMe}(\text{C}_6\text{F}_5)_2$ (**19**). It serves as a $\text{Cp}_2\text{Zr}(\text{H})\text{OTMP}$ zirconocene hydride source in the reaction with CO_2 , giving the respective $[\text{Zr}](\mu\text{-formate})[\text{B}]$ complex **23**. With carbon monoxide it forms the $\text{Zr}(\eta^2\text{-acetaldehyde})[\text{B}]$ complex **30** by transfer of both the hydride and the methyl anion from the Zr/B pair to the carbon atom of the CO molecule.

INTRODUCTION

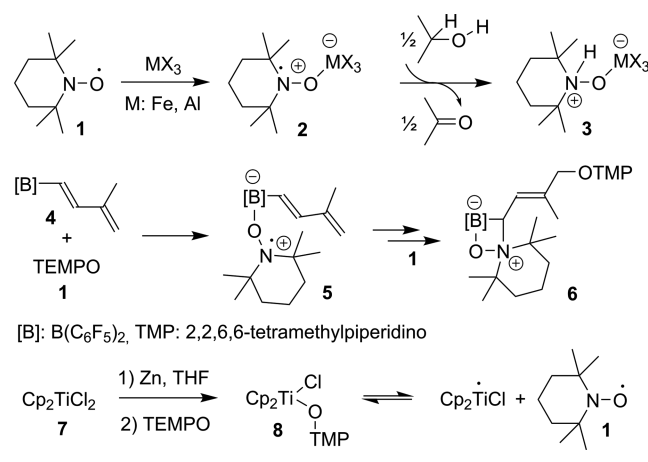
The persistent nitroxide radical 2,2,6,6-tetramethylpiperidine *N*-oxyl (**1**, TEMPO) has found increasing use in organic chemistry.¹ It has also found some interesting applications in organometallic and coordination chemistry. Hoffman et al.² and subsequently Hayton et al.³ had studied the chemistry of various Lewis acid adducts of TEMPO.^{2–4} This revealed a transition from an oxygen to a more nitrogen centered radical upon coordination to Lewis acids BX_3 , AlX_3 , and FeX_3 and related systems. We had used this specific feature to prepare the unique four-membered B,O,N,C-containing heterocycle **6** by reacting the dienylborane **4** with 2 molar equiv of TEMPO (see Scheme 1).⁵ Waymouth et al. described the chemistry of TEMPO-derived titanocene(IV) complexes in a series of reports.⁶ They could show that the TEMPO–titanocene complex **8** was equilibrating with the free TEMPO radical and $\text{Cp}_2\text{Ti}^{\text{III}}\text{Cl}$.

We have now used the TEMPO anion as a stabilizing ligand in zirconocene cation and zirconocene hydride chemistry. This provided an easy entry into zirconocene cation modified frustrated Lewis pair chemistry, which favorably complemented the ongoing development in metallocene-containing FLPs.^{7–9} It also allowed for the ready formation of a reactive zirconocene hydride reagent for CO_2 as well as CO reduction chemistry. The essential findings of this study will be reported in this account.

RESULTS AND DISCUSSION

TEMPO–Zirconocene Cation Generation and Reactions. We used dimethylzirconocene (**9**) as the starting

Scheme 1

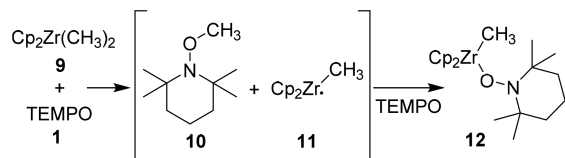


material of our study.¹⁰ It was treated with 2 molar equiv of the persistent nitroxide radical TEMPO **1** (pentane, room temperature, 20 min). The reaction probably proceeds by a formal methyl radical abstraction from the metal complex by a TEMPO equivalent (giving TEMPOMe, which was observed in an in situ NMR experiment; see the Supporting Information for details), followed by trapping of the resulting reactive $\text{Cp}_2\text{Zr}^{\text{III}}\text{Me}$ intermediate **11**¹¹ by a second TEMPO radical to give the product **12**. It was crystallized from the reaction

Received: July 24, 2017

mixture at $-35\text{ }^{\circ}\text{C}$ and isolated in 82% yield as yellow crystals (see Scheme 2).

Scheme 2



At 299 K, compound 12 shows a sharp ^1H NMR Cp signal, methylene resonances, and a broad methyl signal (12 H, relative intensity) of the tetramethylpiperidine group and the $[\text{Zr}]\text{-CH}_3$ ^1H NMR resonance at δ 0.07 (^{13}C : δ 111.0 (Cp), 20.1 ($[\text{Zr}]\text{CH}_3$)).

An X-ray crystal structure analysis of compound 12 (see Figure 1) shows the bent-metallocene unit. The Zr-bound CH_3

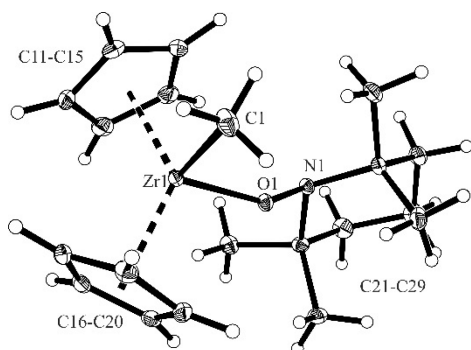
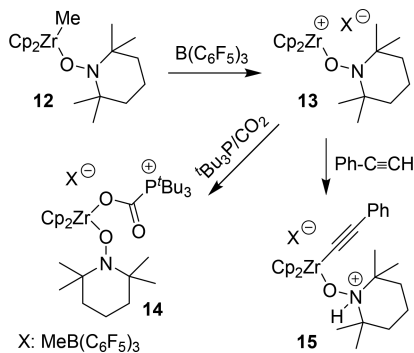


Figure 1. View of the molecular structure of complex 12 (thermal ellipsoids are shown with 15% probability).

group and the $-\text{OTMP}$ (i.e., $-\text{O}-2,2,6,6\text{-tetramethylpiperidino}$) ligand are found in the σ -ligand plane (Zr1–C1 2.286(3) Å, Zr1–O1 1.947(2) Å, C1–Zr1–O1 100.0(1) $^{\circ}$). The Zr1–O1–N1 unit is bent (Zr1–O1–N1 angle 146.5(2) $^{\circ}$, O1–N1 1.436(2) Å) and the nitrogen coordination is trigonal-pyramidal with $\sum\text{N1}^{\text{occ}} = 332.6^{\circ}$.

It is well-known that σ -methyl ligands can be abstracted from the respective zirconocene complexes by treatment with the strong boron Lewis acid $\text{B}(\text{C}_6\text{F}_5)_3$.^{12,13} We used this typical reaction for the preparation of the cationic $[\text{TEMPO}\text{-ZrCp}_2]^+$ complex 13 (see Scheme 3). For that purpose, the neutral $\text{TEMPO}\text{-Zr}(\text{CH}_3)\text{Cp}_2$ precursor 12 was treated with $\text{B}(\text{C}_6\text{F}_5)_3$ ¹⁴ in bromobenzene solution. The resulting red solution

Scheme 3



was stirred for 10 min at room temperature, and then the product was precipitated with pentane. Complex 13 was isolated as a yellow solid in 86% yield. It was characterized by C,H,N elemental analysis and by NMR spectroscopy. The ^1H NMR spectrum (in d_5 -bromobenzene) shows the broad $[\text{B}]\text{-CH}_3$ signal at δ 0.97 (^{13}C : δ 7.3), the typical CH_2 and CH_3 (δ 0.77, 12 H) signals of the O-TMP group, and a sharp Cp signal at δ 6.12 (^{13}C : δ 115.8). The ^{11}B NMR feature of the $[\text{MeB}(\text{C}_6\text{F}_5)_3]^-$ anion occurs at δ -14.1 , and the salt shows the small $\Delta\delta(^{19}\text{F}_{\text{m,p}}) = 3.7$ ppm chemical shift difference typical for such a borate anion situation.¹⁵

The cation 13 can serve as a bulky Lewis acid component in frustrated Lewis pair (FLP) chemistry.^{7–9,16} Typically, it reacts jointly with the bulky $^t\text{Bu}_3\text{P}$ phosphane Lewis base in a cooperative reaction with carbon dioxide (see Scheme 3).¹⁷ In this case, the cation 13 was generated in situ by treating 12 with $\text{B}(\text{C}_6\text{F}_5)_3$ in bromobenzene solution (5 min, room temperature). After adding $^t\text{Bu}_3\text{P}$ to the red solution, the mixture was exposed to a CO_2 atmosphere to give a yellow precipitate of the Zr/P FLP CO_2 trapping product 14. It was isolated as a yellow solid in 75% yield.

An X-ray crystal structure analysis showed the CO_2 molecule trapped between the zirconium cation Lewis acid site and the bulky phosphane Lewis base (see Figure 2). The Zr $^+$ /P pair had

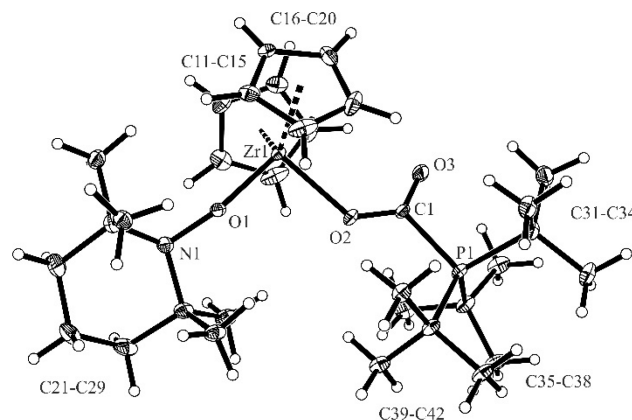


Figure 2. Molecular structure of the Zr $^+$ /P FLP CO_2 addition product 14 (thermal ellipsoids are shown with 15% probability; depicted without the $[\text{MeB}(\text{C}_6\text{F}_5)_3]^-$ anion).

added across one carbon dioxide carbonyl unit. The resulting Zr1–O2 bond (2.163(3) Å) is markedly longer than the adjacent Zr–OTMP bond (Zr1–O1 1.913(3) Å, Zr1–O1–N1 151.5(2) $^{\circ}$). The O2–C1 bond length amounts to 1.261(5) Å, which is markedly longer than the remaining adjacent CO_2 C=O bond (C1–O3 1.209(6) Å); the length of the newly formed C1–P1 bond amounts to 1.898(5) Å. In addition, we see the structure of the spatially separated $[\text{MeB}(\text{C}_6\text{F}_5)_3]^-$ counteranion of product 14.

In CD_2Cl_2 solution at 243 K complex 14 shows the typical NMR signals of the $[\text{Cp}_2\text{Zr}\text{-OTMP}]^+$ core and the $[\text{MeB}(\text{C}_6\text{F}_5)_3]^-$ anion. The ^{13}C NMR signal of the captured CO_2 moiety was located at δ 163.0 (d, $^1J_{\text{PC}} = 83.7$ Hz). Compound 14 shows a ^{31}P NMR feature at δ 47.9 (for details see the Supporting Information).

Complex 13 may even show FLP properties without the aid of an added external Lewis base. It reacts with the terminal alkyne phenylacetylene as an intramolecular Zr $^+$ /N FLP. In bromobenzene solution it reacted readily at room temperature

(20 min) with this alkyne to give the Zr-alkynyl/ammonium product **15**, which was isolated as a solid in 85% yield (see Scheme 3). Its X-ray crystal structure analysis showed (see Figure 3) the attachment of the phenylacetylide σ -ligand at the

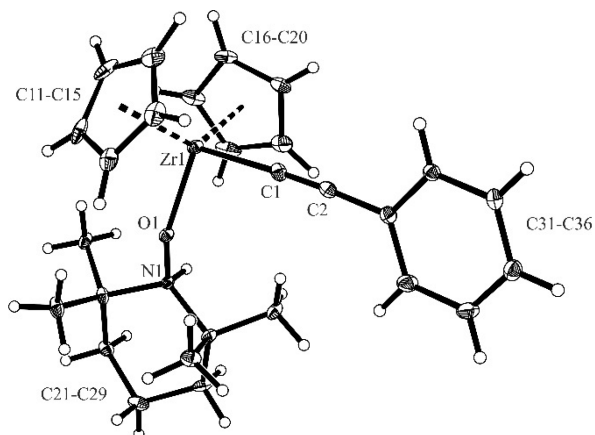


Figure 3. Molecular structure of complex **15** (thermal ellipsoids are shown with 15% probability; depicted without the $\text{MeB}(\text{C}_6\text{F}_5)_3$ anion).

$\text{Cp}_2\text{Zr-OTMP}$ core (Zr1–O1 2.033(2) Å, Zr1–O1–N1 149.5(2)°, Zr1–C1 2.232(4) Å, C1–C2 1.215(6) Å, Zr1–C1–C2 175.7(3)°, C1–Zr1–O1 98.7(2)°). The structure also revealed that the O-TMP nitrogen atom N1 had been protonated, and we observed the pseudotetrahedral $[\text{MeB}(\text{C}_6\text{F}_5)_3]^-$ counteranion.

In solution (CD_2Cl_2) the ammonium proton NMR signal was observed at δ 6.07 (br, s). The Zr-bound σ -acetylide ligand shows ^{13}C NMR resonances at δ 134.6 (ZrC \equiv) and 127.9 (PhC \equiv). We observed the typical NMR features of the $\text{Cp}_2\text{Zr-OTMP}$ unit of the cation and the $[\text{MeB}(\text{C}_6\text{F}_5)_3]^-$ anion (^1H , δ 0.51 (B-Me); ^{11}B , δ –15.0, ^{19}F , $\Delta\delta^{19}\text{F}_{\text{m,p}} = 2.6$ ppm) (for further details see the Supporting Information).

We also generated the $[\text{Cp}_2\text{Zr-OTMP}^+]$ salt by methyl anion abstraction from $\text{Cp}_2\text{Zr}(\text{Me})\text{O-TMP}$ with the trityl cation reagent $[\text{Ph}_3\text{C}^+][\text{B}(\text{C}_6\text{F}_5)_4^-]$.¹⁸ Since we knew that the free zirconocene cation salt did not crystallize well, we trapped it in situ generated (bromobenzene, room temperature, 10 min) with diisopropylcarbodiimide. The trapping reagent was added to the red solution, and we isolated the carbodiimide adduct **17** of the $[\text{Cp}_2\text{Zr-OTMP}^+]$ cation as a yellow solid in 75% yield (see Scheme 4). The X-ray crystal structure analysis showed (see Figure 4) that the $[\text{Cp}_2\text{Zr-OTMP}^+]$ moiety is present in the adduct with typical structural parameters (Zr1–O1 1.930(5) Å, O1–N1 1.450(7) Å, Zr1–O1–N1 147.6(4)°). It has the

Scheme 4

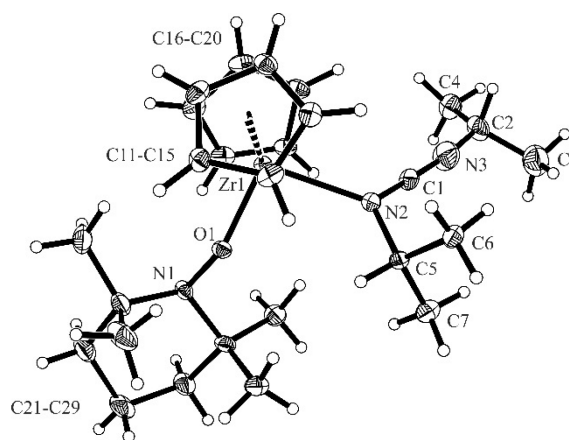
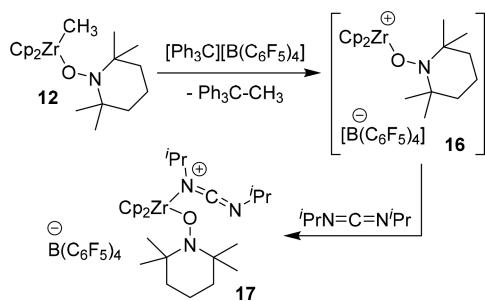


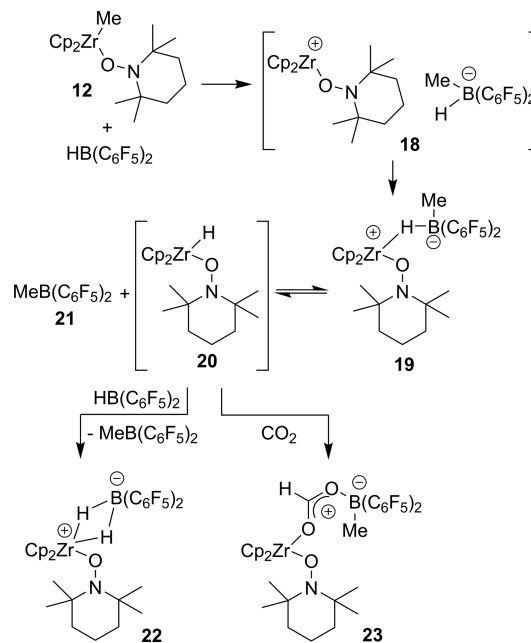
Figure 4. View of the molecular structure of the salt **17** (thermal ellipsoids are shown with 15% probability; depicted without the $\text{B}(\text{C}_6\text{F}_5)_4$ anion).

carbodiimide coordinated in the Cp–Zr–Cp bisecting bent-metallocene σ -ligand plane through the nitrogen atom of one of the $^i\text{PrN}=\text{C}$ units (Zr1–N2 2.319(9) Å, N2–C1 1.213(10) Å, C1–N3 1.178(11) Å, N2–C1–N3 175(3)°, O1–Zr1–N2 96.6(5)°, Zr1–O1–N1 147.6(4)°). The counteranion is $[\text{B}(\text{C}_6\text{F}_5)_4]^-$.

In solution, we observed the $^1\text{H}/^{13}\text{C}$ NMR signals of a pair of isopropyl substituents at the carbodiimide nitrogen atoms in addition to the typical NMR features of the bent metallocene and its –OTMP σ -ligand. The $[\text{B}(\text{C}_6\text{F}_5)_4]^-$ anion shows a ^{11}B NMR resonance at δ –16.9 (for further details about the characterization of complex **17** see the Supporting Information).

TEMPO-Derived Zirconium Hydride Reactions. For the introduction of a reactive hydride functionality, we reacted the TEMPO-derived $\text{Cp}_2\text{Zr}(\text{CH}_3)\text{-OTMP}$ complex **12** with Piers' borane $[\text{HB}(\text{C}_6\text{F}_5)_2]^{19}$ in two different stoichiometries (see Scheme 5). We first reacted complex **12** with 1 molar equiv of

Scheme 5



HB(C₆F₅)₂. The reaction mixture in toluene was stirred for 30 min at room temperature, and then the resulting product **19** was precipitated with pentane. It was isolated in 71% yield. The X-ray crystal structure analysis (see Figure 5) revealed that the

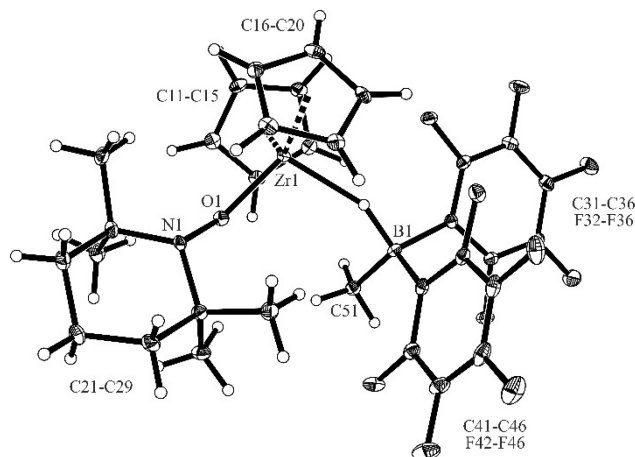


Figure 5. Molecular structure of the μ -H-bridged tight ion pair **19** (thermal ellipsoids are shown with 30% probability). Selected bond lengths (Å) and angles (deg): Zr1–O1 1.949(2), O1–N1 1.446(3), B1–C51 1.622(4), Zr1–O1–N1 143.1(2), \sum N1^{occ} 333.3, \sum B1^{occ} 335.8, B1...Zr1 3.270 Å.

borane HB(C₆F₅)₂ had served as a typical strong boron Lewis acid and abstracted the methyl anion equivalent from zirconium. However, the components of the formally resulting salt **18** were then combined to give a tight ion pair, as is often observed in zirconocene cation chemistry,²⁰ in this case forming the hydride-bridged species **19**. It features the bulky H-B(Me)(C₆F₅)₂ anion hydride-bonded to zirconium in the bent-metallocene σ -ligand plane. The –OTMP σ -ligand is occupying the other available σ -ligand site, but the bulky TMP group itself is slightly rotated out of the Cp–Zr–Cp bisecting plane toward one of the Cp ligands.

In bromobenzene-*d*₅ (299 K) solution we observed the [B]–H–[Zr] ¹H NMR hydride signal at δ –0.98 and the nonbridging [B]–CH₃ resonance at δ 0.90 (¹³C: δ 7.3) in addition to the Cp₂Zr resonance (δ 6.18, s, 10 H) and the typical ¹H/¹³C NMR signals of the Zr- σ -OTMP ligand. The (μ -H)BMe-(C₆F₅)₂ anion section of compound **19** shows a ¹¹B NMR resonance at δ –8.0 and a $\Delta\delta$ (¹⁹F_{m,p}) = 5.0 ppm chemical shift separation of the *m*- and *p*-fluorine signals of the pair of C₆F₅ groups at boron.

The B–H linker in compound **19** can readily be broken (probably reversibly) to generate compounds **20** and **21**. Compound **21** was observed directly, but compound **20** was detected by formation of its trapping product **22** with HB(C₆F₅)₂. We prepared compound **22** either by treatment of the general starting material **12** directly with 2 molar equiv of HB(C₆F₅)₂ or by the reaction of the in situ generated Zr–H–B complex **19** with 1 molar equiv of Piers' borane [HB(C₆F₅)₂]. The former reaction mixture was stirred for 30 min at room temperature in toluene. Subsequent workup by layering with pentane and crystallization at –35 °C (2 days) eventually gave the Zr-(μ -H)₂-B complex **22** as a crystalline material in 91% yield. The crystals were suitable for a structure determination by X-ray diffraction (see Figure 6). It shows the attachment of the (μ -H)₂B(C₆F₅)₂ moiety to zirconium in the bent-metallocene σ -ligand plane. Naturally, the bridging hydrides

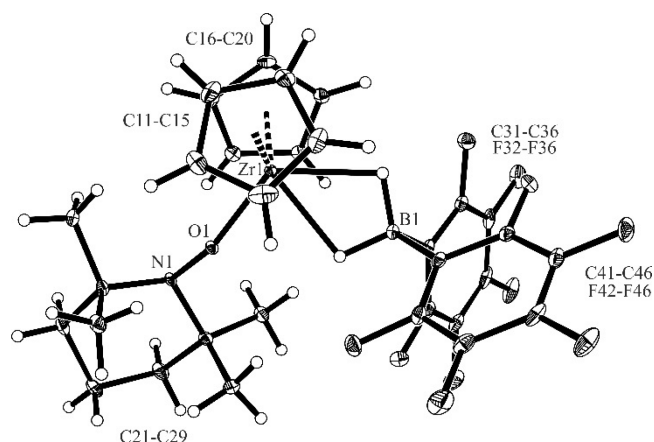


Figure 6. Projection of the molecular structure of complex **22** (thermal ellipsoids are shown with 30% probability). Selected bond lengths (Å) and angles (deg): Zr1–O1 1.951(2), O1–N1 1.443(2), B1–C31 1.618(3), B1–C41 1.623(3), Zr1–O1 146.9(1), \sum N1^{occ} 333.0, B1...Zr1 2.703(2).

occupy two of the three principally available binding sites, one laterally and one centrally oriented.^{21,22} The remaining lateral site in this coordination plane in front of the bent-metallocene wedge is taken by the –O-TMP σ -ligand.

The ¹H NMR spectrum of compound **22** (dichloromethane-*d*₂, 193 K) shows a pair of [B]–H₂–[Zr] resonances at δ 1.75 and 0.05, respectively. We found two sharp Cp singlets at δ 6.33 and 6.15 (¹³C: δ 113.5, 112.5) and two sets of ¹⁹F NMR signals of the pair of C₆F₅ substituents at boron (¹¹B: δ –22.7 (t, ¹J_{BH} \approx 70 Hz)) (for further details see the Supporting Information).

The zirconium hydride/CH₃B(C₆F₅)₂ mixture (**20/21**) traps carbon dioxide. We generated the precursor complex **19** in situ by treatment of compound **12** with 1 molar equiv of HB(C₆F₅)₂ in toluene solution and trapped the **20/21** pair from its endergonic equilibrium by exposure to a CO₂ atmosphere. The red solution turned yellow, and we isolated the formate complex **23** as a yellow crystalline solid in 90% yield. The ¹H NMR spectrum (dichloromethane-*d*₂, 248 K) showed the signals of the newly formed formate moiety at δ 8.51 (¹H) and δ 174.9 (¹³C), respectively. In addition, we have monitored the NMR features of the Zr-bonded σ -OTMP ligand, the bent-metallocene unit (δ 6.37, (¹H, s, 10H), δ 114.5 (¹³C)) and the –B(CH₃)(C₆F₅)₂ moiety (δ 0.56 (¹H, CH₃), δ 8.7 (¹³C, CH₃), δ 3.2 (¹¹B (299 K), $\Delta\delta$ (¹⁹F_{m,p}) = 4.9 ppm (C₆F₅ at boron)).

The X-ray crystal structure analysis (see Figure 7) confirmed the formation of the formate group by hydride reduction of CO₂, which was found to be bridging between zirconium and boron. The Zr1-(HCO₂)-B1 unit shows a sickle-shaped arrangement with dihedral angles θ (Zr1–O2–C1–O3) = –0.4(7)° and θ (O2–C1–O3–B1) = 178.2(4)°, respectively. The O2–C1 (1.241(4) Å) and C1–O3 (1.253(4) Å) bonds are very similar in length, which indicates a largely delocalized structure. The Cp₂Zr–OTMP and MeB(C₆F₅)₂ units exhibit the usual bonding parameters.

Formylborane and formylborate complexes are quite rare.²³ The few recently reported examples are shown in Scheme 6. The complexes **24** and **25**, which were reported by Stephan et al.^{24a} and Piers et al.,^{24b} respectively, are somewhat labile. They react further by C₆F₅ migration from boron to carbon. We had prepared the neutral genuine formylborane **26** by CO reduction with HB(C₆F₅)₂ at vicinal P/B FLP templates

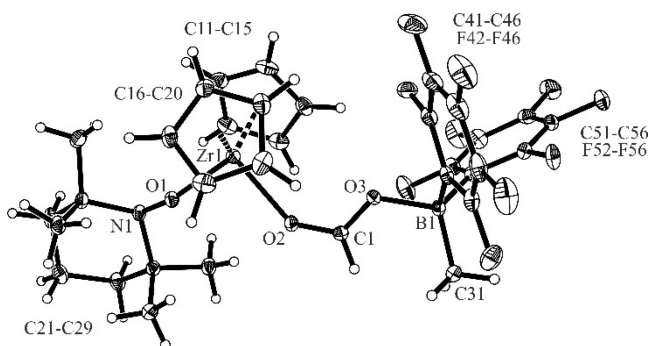
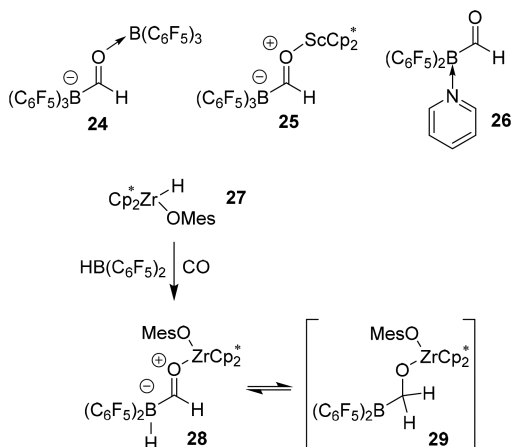


Figure 7. View of the molecular structure of the Zr-formate complex **23** (thermal ellipsoids are shown with 15% probability). Selected bond lengths (Å) and angles (deg): Zr1–O1 1.935(3), O1–N1 1.439(4), Zr1–O2 2.154(3), O3–B1 1.587(5), Zr1–O1–N1 146.9(2), Zr1–O2–C1 139.4(3), O2–C1–O3 123.2(4), C1–O3–B1 125.2(3), $\sum B1^{ccc}$ 337.8, $\sum N1^{ccc}$ 332.9.

Scheme 6



followed by cleavage with pyridine derivatives.²⁵ We recently also reported the preparation and isolation of the Zr-stabilized formyl hydridoborate **28**, which equilibrated with the endergonic [B]–CH₂–O–[Zr] isomer **29**.²⁶ In view of these reports it was tempting to use the incipient zirconium hydride/borane pair **20/21** for CO reduction. We generated the Zr/B complex **19** in situ as usual and then exposed the red solution to a CO atmosphere (1.5 bar, room temperature, 2 h, in toluene). Subsequent layering with pentane and storing for 4 days at –35 °C produced crystals of compound **30**, which were isolated in 61% yield.

The X-ray crystal structure analysis (see Figure 8) revealed that the CO molecule had added both the hydride and the methyl group from the equilibrating **19** ⇌ **20** + **21** pair to produce an acetaldehyde moiety, which was found to be oxygen-bridged between zirconium and boron. The newly formed MeCHO unit is found η^2 -bonded through both oxygen and carbon to the B(C₆F₅)₂ group, and it is O-coordinated to zirconium. The three-membered heterocycle has a saturated borataoxirane-type structure with all three core bonds being in the respective σ -bond range (B1–O2 1.530(4) Å, B1–C1 1.547(4) Å, and O2–C1 1.515(4) Å). The carbon atom C1 has the methyl group and the hydrogen atom originating from the reagent **19** bonded to it.

The newly formed chiral center of complex **30** gives rise to a ¹H NMR (benzene-*d*₆, 299 K) doublet (δ 1.30, CH₃) and a

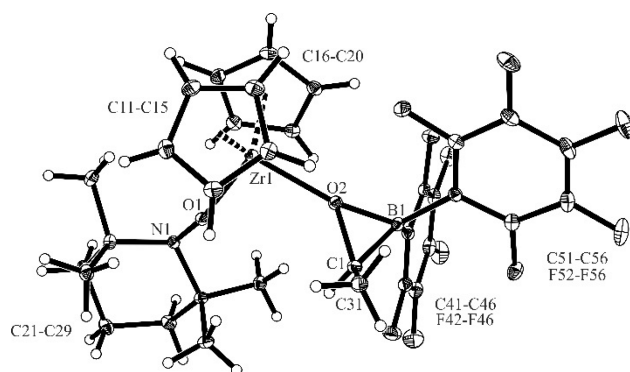
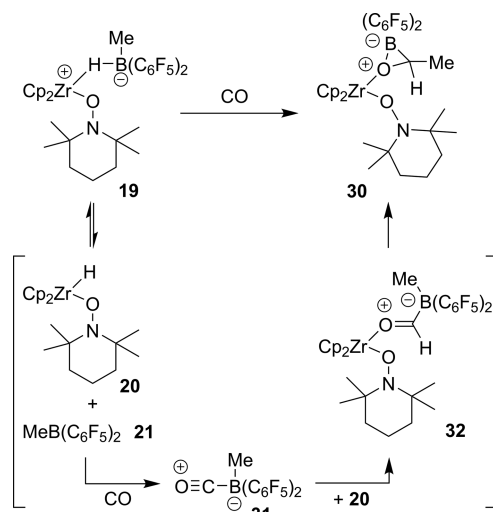


Figure 8. View of the molecular structure of the CO-reduction product **30** (thermal ellipsoids are shown with 15% probability). Selected bond lengths (Å) and angles (deg): Zr1–O1 1.938(2), O1–N1 1.438(3), Zr1–O2 2.142(2), C1–C31 1.499(5), B1–C41 1.617(5), B1–C51 1.619(5), Zr1–O1–N1 147.9(2), Zr1–O2–B1 161.5(2), Zr1–O2–C1 134.6(2), O1–Zr1–O2 99.7(1).

quartet (δ 4.16, CH). The CO-derived carbon atom shows a ¹³C NMR resonance at δ 74.0 (broad). We observe the ¹⁹F NMR signals of a pair of diastereotopic C₆F₅ substituents at zirconium (¹H δ 6.05 and 5.99 and ¹³C δ 115.1 and δ 113.9, respectively). Compound **30** shows a ¹¹B NMR feature at δ –7.6.

There are several mechanistic pathways conceivable for the formation of complex **30** from **19** + CO. At this time we do not have solid evidence in favor of one or another, but in view of our recent findings of the formation of the formylborate complex **28** and its chemistry (see Scheme 6 and the respective literature) we find the putative pathway outlined in Scheme 7

Scheme 7



an attractive option. This involves CO addition to the CH₃B(C₆F₅)₂ compound **21**^{27,28} of the endergonic **19** ⇌ **20** + **21** equilibrium followed by zirconium hydride reduction of the resulting borane carbonyl **31** to generate the formylborate intermediate **32**. Methyl migration from boron to the carbonyl carbon atom then could close the reaction sequence, leading to the observed product **30**. An alternative reaction pathway with an inverted sequence of elemental reaction steps cannot be ruled out at this time.

CONCLUSIONS

Waymouth et al. had used the TEMPO radical as an active ligand in titanium(III) chemistry.⁶ They had shown that $\text{Cp}_2\text{Ti}(\text{Cl})\text{-OTMP}$ was in an equilibrium with Cp_2TiCl and the free TEMPO radical. We have now used the TEMPO radical in a different way. The reaction of Cp_2ZrMe_2 with TEMPO proceeded by means of a methyl radical abstraction with rapid subsequent trapping of the alleged Zr(III) intermediate by a second TEMPO radical equivalent to give the stable $\text{Cp}_2\text{Zr}(\text{Me})\text{-OTMP}$ complex **12**. Since this contained an active Zr- CH_3 σ -ligand, the situation was set for methyl anion abstraction by active boron Lewis acids, a common method of zirconocene cation formation, which have been used ubiquitously in bent metallocene Ziegler–Natta catalysis chemistry.^{12,13} In our case two rather different areas of chemistry could be addressed in this way which differed substantially depending on the strong boron Lewis acid used for methyl anion equivalent abstraction: the reaction with $\text{B}(\text{C}_6\text{F}_5)_3$ generated the $[\text{Cp}_2\text{Zr-OTMP}^+]$ cation, which showed some frustrated Lewis pair (FLP) features. It served as an intramolecular Zr^+/N FLP toward the terminal alkyne phenylacetylene, in which the TMP nitrogen serves as the Lewis base component to react jointly with its Zr^+ Lewis acid counterpart.²⁹ In the presence of the bulky $^t\text{Bu}_3\text{P}$ Lewis base the $[\text{Cp}_2\text{Zr-OTMP}^+]$ cation serves as the Lewis acid of an intermolecular FLP, in our case active for CO_2 binding.

In contrast, methyl anion abstraction from $\text{Cp}_2\text{Zr}(\text{Me})\text{-OTMP}$ by the Lewis acidic $\text{HB}(\text{C}_6\text{F}_5)_2$ borane led to a hydride-bridged $[\text{Zr}]\text{-H-}[\text{B}]$ tight ion pair that apparently equilibrated with an active zirconium hydride by $\text{H}\cdots[\text{B}]$ bond rupture. This reaction mode became visible in the active reduction of CO_2 to a $[\text{Zr}]\text{-(}\mu\text{-formate)-}[\text{B}]$ product or in the reduction of carbon monoxide to give the $[\text{Zr}]\text{-(}\eta^2\text{-acetaldehyde)-}[\text{B}]$ product **30**. The latter chemistry is reminiscent of that of our previously described formyl hydridoborato Zr complex **28**. However, compound **28** is the stable, isolable isomer in its series and the internal hydride addition product **29** was only trapped by added reagents. In our new Zr(TEMPO)-derived system the situation is different: here we isolated the η^2 -aldehyde Zr complex and its formyl (or alternatively acetyl) precursors only have a fleeting existence.

The reactions of the $\text{Cp}_2\text{Zr}(\text{Me})\text{OTMP}$ starting material with $\text{B}(\text{C}_6\text{F}_5)_3$ or $\text{HB}(\text{C}_6\text{F}_5)_2$ represent a remarkable dichotomy of complementary reaction modes having become available by a simple switching between a pair of conceptually related boron Lewis acids. This may indicate the versatility of the group 4 organometallic starting material brought about by the use of the σ -OTMP ligand that was so easily introduced by means of the TEMPO radical pathway.

EXPERIMENTAL SECTION

For general information and the spectroscopic and structural data of these new compounds, see the [Supporting Information](#).

Preparation of Complex 12. Dimethylzirconocene Cp_2ZrMe_2 (250 mg, 1.00 mmol) was added to a solution of TEMPO (320.0 mg, 2.0 mmol) in pentane (1.0 mL). The reaction mixture was stirred at room temperature for 20 min, and then the resulting pale yellow mixture was stored at ca. -35°C overnight. The formed yellow solid was isolated by filtration, washed with cold pentane (2×0.5 mL), and dried in vacuo to give compound **12** (321 mg, 0.82 mmol, 82%). Crystals suitable for an X-ray single-crystal structure analysis were obtained from a pentane solution of compound **12** at -35°C . Anal. Calcd for $\text{C}_{20}\text{H}_{31}\text{NOZr}$: C, 61.17; H, 7.96, N, 3.57. Found: C, 60.32; H, 7.93, N, 3.64.

Preparation of Complex 13. Tris(pentafluorophenyl)borane (102.4 mg, 0.20 mmol) was added to a solution of compound **12** (78.4 mg, 0.20 mmol) in bromobenzene (0.8 mL). After the red mixture was stirred for 10 min at room temperature, the resulting solution was covered with pentane (ca. 18 mL) and stirred at room temperature for 15 min. Compound **13** precipitated from the solution as a yellow solid, which was collected and dried in vacuo (155.3 mg, 0.17 mmol, 86%). Anal. Calcd for $\text{C}_{38}\text{H}_{31}\text{BF}_{15}\text{NOZr}$: C, 50.45; H, 3.45, N, 1.55. Found: C, 50.31; H, 3.37, N, 1.66.

Preparation of Complex 14. Tris(pentafluorophenyl)borane (102.4 mg, 0.20 mmol) was added to a solution of compound **12** (78.4 mg, 0.20 mmol) in bromobenzene (0.6 mL). After the red mixture was stirred for 5 min at room temperature, P^tBu_3 (40.4 mg, 0.20 mmol) was added. Then the Schlenk flask was carefully evacuated and exposed to CO_2 (1.5 bar). The mixture turned yellow immediately. Then pentane (ca. 15 mL) was added with vigorous stirring at room temperature to give a yellow precipitate, which was collected and dried in vacuo. Compound **14** was obtained as a yellow powder (172.1 mg, 0.15 mmol, 75%). Single crystals suitable for an X-ray crystal structure analysis were obtained by slow diffusion of pentane into a solution of compound **14** in CH_2Cl_2 at -35°C . Anal. Calcd for $\text{C}_{51}\text{H}_{38}\text{BF}_{15}\text{NO}_3\text{PZr}$: C, 53.22; H, 5.08, N, 1.22. Found: C, 52.40; H, 4.75, N, 0.99.

Preparation of Complex 15. Tris(pentafluorophenyl)borane (102.4 mg, 0.20 mmol) was added to a solution of compound **12** (78.4 mg, 0.20 mmol) in bromobenzene (0.6 mL) to give a red solution, which was stirred for 10 min at room temperature before phenylacetylene (20.4 mg, 0.20 mmol) was added. The reaction mixture changed from red to yellow. After it was stirred for 20 min at room temperature, the yellow solution was covered with pentane (ca. 20 mL) and stirred vigorously at room temperature for 20 min. Compound **15** precipitated from the solution as a yellow solid, which was collected and then washed with Et_2O (1.0 mL). After removal of all volatiles in vacuo, compound **15** was obtained as a yellow powder (171.2 mg, 0.17 mmol, 85%). Single crystals suitable for an X-ray crystal structure analysis were obtained by slow diffusion of pentane into a solution of compound **15** in CH_2Cl_2 at -35°C . Anal. Calcd for $\text{C}_{46}\text{H}_{37}\text{BF}_{15}\text{NOZr}$: C, 54.88; H, 3.70, N, 1.39. Found: C, 53.13; H, 3.50, N, 1.80.

Preparation of Complex 17. $[\text{Ph}_3\text{C}][\text{B}(\text{C}_6\text{F}_5)_4]$ (92.2 mg, 0.10 mmol) was added to a solution of compound **12** (39.2 mg, 0.10 mmol) in bromobenzene (0.6 mL). The red solution was stirred for 10 min at room temperature before N,N' -diisopropylcarbodiimide (12.6 mg, 0.10 mmol) was added. The color of the reaction mixture gradually changed from red to yellow. After ca. 30 min pentane (ca. 15 mL) was added and the yellow solution was stirred at room temperature for 10 min. The formed yellow precipitate was collected and dried in vacuo to give compound **17** (88.7 mg, 0.075 mmol, 75%). Single crystals suitable for an X-ray crystal structure analysis were obtained by slow diffusion of pentane into a solution of compound **17** in CH_2Cl_2 at -35°C . Anal. Calcd for $\text{C}_{50}\text{H}_{42}\text{BF}_{20}\text{N}_3\text{OZr}$: C, 50.77; H, 3.58, N, 3.55. Found: C, 50.24; H, 3.21, N, 3.53.

Preparation of Complex 19. Bis(pentafluorophenyl)borane $\text{HB}(\text{C}_6\text{F}_5)_2$ (69.0 mg, 0.20 mmol) was added to a solution of compound **12** (78.4 mg, 0.20 mmol) in toluene (0.5 mL). After the red reaction mixture was stirred for 30 min at room temperature, it was covered with pentane (ca. 10 mL). A yellow precipitate was formed after storage of the solution for 1 day at ca. -35°C . The solid was collected, and all volatiles were removed in vacuo to finally give a yellow solid (104.1 mg, 0.14 mmol, 71%). Single crystals suitable for an X-ray crystal structure analysis were obtained by slow diffusion of pentane into a solution of compound **19** in toluene at -35°C . Anal. Calcd for $\text{C}_{32}\text{H}_{32}\text{BF}_{10}\text{NOZr}$: C, 52.04; H, 4.37, N, 1.90. Found: C, 52.46; H, 4.23, N, 1.62.

Preparation of Complex 22. Bis(pentafluorophenyl)borane $\text{HB}(\text{C}_6\text{F}_5)_2$ (138.0 mg, 0.40 mmol) was added to a solution of compound **12** (78.4 mg, 0.20 mmol) in toluene (0.5 mL). After the reaction mixture was stirred for 30 min at room temperature, the resulting yellow solution was covered with pentane (ca. 10 mL) and stored at ca. -35°C for 2 days. Finally, compound **22** (132.0 mg, 0.18

mmol, 91%) was isolated as yellow crystals, which were suitable for an X-ray single-crystal structure analysis. Anal. Calcd for $C_{31}H_{30}BF_{10}NOZr$: C, 51.38; H, 4.17, N, 1.93. Found: C, 51.29; H, 3.87, N, 1.79.

Preparation of Complex 23. Bis(pentafluorophenyl)borane (69.0 mg, 0.20 mmol) was added to a solution of compound 12 (78.4 mg, 0.20 mmol) in toluene (0.50 mL) to give a red solution. After the mixture was stirred for 15 min at room temperature, the Schlenk tube was carefully evacuated and exposed to CO_2 (1.5 bar). The mixture immediately turned yellow. After the resulting solution was stirred for 30 min at room temperature, it was covered with pentane (ca. 10 mL) and stored at ca. $-35^\circ C$. After 2 days yellow crystals were formed (142.2 mg, 0.18 mmol, 90%), which were suitable for an X-ray single-crystal structure analysis. Anal. Calcd for $C_{33}H_{32}BF_{10}NO_3Zr$: C, 50.64; H, 4.12, N, 1.79. Found: C, 50.06; H, 3.83, N, 1.57.

Preparation of Complex 30. Bis(pentafluorophenyl)borane (138.0 mg, 0.40 mmol) was added to a solution of compound 12 (156.8 mg, 0.40 mmol) in toluene (1.0 mL) to give a red solution. After the mixture was stirred for 15 min at room temperature, the Schlenk tube was carefully evacuated and the solution was exposed to CO (1.5 bar). The mixture immediately turned yellow. After the solution was stirred for 2 h at room temperature, it was covered with pentane (ca. 18 mL) and stored at ca. $-35^\circ C$. After 4 days yellow crystals were formed and isolated (183.1 mg, 0.24 mmol, 61%). The obtained crystals were suitable for an X-ray single-crystal structure analysis. Anal. Calcd for $C_{33}H_{32}BF_{10}NO_2Zr$: C, 51.70; H, 4.21, N, 1.83. Found: C, 51.94; H, 4.22, N, 1.74.

■ ASSOCIATED CONTENT

Supporting Information

The Supporting Information is available free of charge on the ACS Publications website at DOI: 10.1021/acs.organomet.7b00558.

Experimental and analytical details and characterization data (PDF)

Accession Codes

CCDC 1564042–1564049 contain the supplementary crystallographic data for this paper. These data can be obtained free of charge via www.ccdc.cam.ac.uk/data_request/cif, or by emailing data_request@ccdc.cam.ac.uk, or by contacting The Cambridge Crystallographic Data Centre, 12 Union Road, Cambridge CB2 1EZ, UK; fax: +44 1223 336033.

■ AUTHOR INFORMATION

Corresponding Author

*E-mail for G.E.: erker@uni-muenster.de.

ORCID

Gerald Kehr: 0000-0002-5196-2491

Gerhard Erker: 0000-0003-2488-3699

Notes

The authors declare no competing financial interest.

■ ACKNOWLEDGMENTS

Financial support from Deutsche Forschungsgemeinschaft and the Alexander von Humboldt-Stiftung (stipend to Y.-L.L.) is gratefully acknowledged.

■ REFERENCES

(1) For reviews, see: (a) Sheldon, R. A.; Arends, I. W. C. E. *Adv. Synth. Catal.* **2004**, *346*, 1051–1071. (b) Vogler, T.; Studer, A. *Synthesis* **2008**, *2008*, 1979–1993. (c) Tebben, L.; Studer, A. *Angew. Chem., Int. Ed.* **2011**, *50*, 5034–5068.

(2) (a) Hoffman, B. M.; Eames, T. B. *J. Am. Chem. Soc.* **1969**, *91*, 5168–5170. (b) Hoffman, B. M.; Eames, T. B. *J. Am. Chem. Soc.* **1971**, *93*, 3141–3146.

(3) (a) Scepianiak, J. J.; Wright, A. M.; Lewis, R. A.; Wu, G.; Hayton, T. W. *J. Am. Chem. Soc.* **2012**, *134*, 19350–19353. (b) Nguyen, T.-A. D.; Wright, A. M.; Page, J. S.; Wu, G.; Hayton, T. W. *Inorg. Chem.* **2014**, *53*, 11377–11387.

(4) Wright, A. M.; Page, J. S.; Scepianiak, J. J.; Wu, G.; Hayton, T. W. *Eur. J. Inorg. Chem.* **2013**, *2013*, 3817–3820.

(5) Türkyilmaz, F.; Kehr, G.; Li, J.; Daniliuc, C. G.; Tesch, M.; Studer, A.; Erker, G. *Angew. Chem., Int. Ed.* **2016**, *55*, 1470–1473.

(6) (a) Mahanthappa, M. K.; Huang, K.-W.; Cole, A. P.; Waymouth, R. M. *Chem. Commun.* **2002**, 502–503. (b) Huang, K.-W.; Waymouth, R. M. *J. Am. Chem. Soc.* **2002**, *124*, 8200–8201. (c) Huang, K.-W.; Waymouth, R. M. *Dalton Trans* **2004**, 354–356. (d) Huang, K.-W.; Han, J. H.; Cole, A. P.; Musgrave, C. B.; Waymouth, R. M. *J. Am. Chem. Soc.* **2005**, *127*, 3807–3816. (e) Huang, K.-W.; Han, J. H.; Musgrave, C. B.; Waymouth, R. M. *Organometallics* **2006**, *25*, 3317–3323. (f) DeBeer George, S.; Huang, K.-W.; Waymouth, R. M.; Solomon, E. I. *Inorg. Chem.* **2006**, *45*, 4468–4477. (g) Son, K.-S.; Jöge, F.; Waymouth, R. M. *Macromolecules* **2008**, *41*, 9663–9668. (h) Dove, A. P.; Kiesewetter, E. T.; Ottenwaelder, X.; Waymouth, R. M. *Organometallics* **2009**, *28*, 405–412.

(7) Neu, R. C.; Otten, E.; Lough, A.; Stephan, D. W. *Chem. Sci.* **2011**, *2*, 170–176.

(8) (a) Chapman, A. M.; Haddow, M. F.; Wass, D. F. *J. Am. Chem. Soc.* **2011**, *133*, 8826–8829. (b) Chapman, A. M.; Haddow, M. F.; Wass, D. F. *J. Am. Chem. Soc.* **2011**, *133*, 18463–18478. (c) Flynn, S. R.; Wass, D. F. *ACS Catal.* **2013**, *3*, 2574–2581. (d) Metters, O. J.; Forrest, S. J. K.; Sparkes, H. A.; Manners, I.; Wass, D. F. *J. Am. Chem. Soc.* **2016**, *138*, 1994–2003. (e) Flynn, S. R.; Metters, O. J.; Manners, I.; Wass, D. F. *Organometallics* **2016**, *35*, 847–850. (f) Metters, O. J.; Flynn, S. R.; Dowds, C. K.; Sparkes, H. A.; Manners, I.; Wass, D. F. *ACS Catal.* **2016**, *6*, 6601–6611. (g) Chapman, A. M.; Flynn, S. R.; Wass, D. F. *Inorg. Chem.* **2016**, *55*, 1017–1021.

(9) (a) Xu, X.; Kehr, G.; Daniliuc, C. G.; Erker, G. *Angew. Chem., Int. Ed.* **2013**, *52*, 13629–13632. (b) Xu, X.; Kehr, G.; Daniliuc, C. G.; Erker, G. *Organometallics* **2013**, *32*, 7306–7311. (c) Xu, X.; Kehr, G.; Daniliuc, C. G.; Erker, G. *J. Am. Chem. Soc.* **2013**, *135*, 6465–6476. (d) Fromel, S.; Kehr, G.; Fröhlich, R.; Daniliuc, C. G.; Erker, G. *Dalton Trans.* **2013**, *42*, 14531–14536. (e) Xu, X.; Kehr, G.; Daniliuc, C. G.; Erker, G. *J. Am. Chem. Soc.* **2014**, *136*, 12431–12443. (f) Xu, X.; Kehr, G.; Daniliuc, C. G.; Erker, G. *J. Am. Chem. Soc.* **2015**, *137*, 4550–4557. (g) Xu, X.; Kehr, G.; Daniliuc, C. G.; Erker, G. *Organometallics* **2015**, *34*, 2655–2661. (h) Normand, A. T.; Daniliuc, C. G.; Wibbeling, B.; Kehr, G.; Le Gendre, P.; Erker, G. *J. Am. Chem. Soc.* **2015**, *137*, 10796–10808. (i) Jian, Z.; Daniliuc, C. G.; Kehr, G.; Erker, G. *Organometallics* **2017**, *36*, 424–434.

(10) (a) Wailes, P. C.; Weigold, H.; Bell, A. P. *J. Organomet. Chem.* **1972**, *34*, 155–164. (b) Samuel, E.; Rausch, M. D. *J. Am. Chem. Soc.* **1973**, *95*, 6263–6267. (c) Xu, X.; Fröhlich, R.; Daniliuc, C. G.; Kehr, G.; Erker, G. *Chem. Commun.* **2012**, *48*, 6109–6111.

(11) For a review, see: (a) Lancaster, S. J. In *Comprehensive Organometallic Chemistry III*; Crabtree, R. H., Mingos, D. M. P., Eds.; Bochmann, M., Vol. Ed.; Elsevier: Oxford, U.K., 2007; Vol. 4, Chapter 4.07, pp 741–757. For selected examples of Zr(III) compound, see: (b) Benard, M.; Rohmer, M.-M. *J. Am. Chem. Soc.* **1992**, *114*, 4785–4790. (c) Fryzuk, M. D.; Mylvaganam, M. *J. Am. Chem. Soc.* **1993**, *115*, 10360–10361. (d) Soleil, F.; Choukroun, R. *J. Am. Chem. Soc.* **1997**, *119*, 2938–2939. (e) Lenton, T. N.; Bercaw, J. E.; Panchenko, V. N.; Zakharov, V. A.; Babushkin, D. E.; Soshnikov, I. E.; Talsi, E. P.; Brintzinger, H. H. *J. Am. Chem. Soc.* **2013**, *135*, 10710–10719.

(12) (a) Tjaden, E. B.; Swenson, D. C.; Jordan, R. F. *Organometallics* **1995**, *14*, 371–386. (b) Carr, A. G.; Dawson, D. M.; Bochmann, M. *Macromolecules* **1998**, *31*, 2035–2040. (c) Beswick, C. L.; Marks, T. J. *Organometallics* **1999**, *18*, 2410–2412. (d) Carpentier, J.-F.; Wu, Z.; Lee, C. W.; Strömberg, S.; Christopher, J. N.; Jordan, R. F. *J. Am. Chem. Soc.* **2000**, *122*, 7750–7767. (e) Beswick, C. L.; Marks, T. J. *J. Am. Chem. Soc.* **2000**, *122*, 10358–10370. (f) Li, L.; Stern, C. L.;

Marks, T. J. *Organometallics* **2000**, *19*, 3332–3337. (g) Chen, M.-C.; Roberts, J. A. S.; Marks, T. J. *J. Am. Chem. Soc.* **2004**, *126*, 4605–4625.

(13) For reviews, see: (a) Bochmann, M. *Organometallics* **2010**, *29*, 4711–4740. (b) Bochmann, M. *Acc. Chem. Res.* **2010**, *43*, 1267–1278.

(14) For some selected examples, see: (a) Sassmannshausen, J. *Organometallics* **2000**, *19*, 482–489. (b) Landis, C. R.; Rosaaen, K. A.; Sillars, D. R. *J. Am. Chem. Soc.* **2003**, *125*, 1710–1711. (c) Stahl, N. G.; Salata, M. R.; Marks, T. J. *J. Am. Chem. Soc.* **2005**, *127*, 10898–10909. (d) Choukroun, R.; Wolff, F.; Lorber, C.; Donnadieu, B. *Organometallics* **2003**, *22*, 2245–2248. (e) Strauch, J. W.; Fauré, J.-L.; Bredeau, S.; Wang, C.; Kehr, G.; Fröhlich, R.; Luftmann, H.; Erker, G. *J. Am. Chem. Soc.* **2004**, *126*, 2089–2104.

(15) For early reports on the discussion of the relationship of coordination environment toward boron and ^{19}F NMR resonances, see: (a) Horton, A. D.; de With, J. *Organometallics* **1997**, *16*, 5424–5436. (b) Parks, D. J.; Blackwell, J. M.; Piers, W. E. *J. Org. Chem.* **2000**, *65*, 3090–3098. For selected leading examples of the typical NMR scale of $\Delta\delta(^{19}\text{F}_{\text{m,p}})$ values of $\text{RB}(\text{C}_6\text{F}_5)_3^-$ tetracoordinated borate systems, see: (c) Welch, G. C.; Juan, R. R. S.; Masuda, J. D.; Stephan, D. W. *Science* **2006**, *314*, 1124–1126. (d) Spies, P.; Erker, G.; Kehr, G.; Bergander, K.; Fröhlich, R.; Grimme, S.; Stephan, D. W. *Chem. Commun.* **2007**, 5072–5074.

(16) For reviews of frustrated Lewis pair (FLP) chemistry, see: (a) Stephan, D. W.; Erker, G. *Angew. Chem., Int. Ed.* **2010**, *49*, 46–76. (b) Stephan, D. W.; Erker, G. *Angew. Chem., Int. Ed.* **2015**, *54*, 6400–6441. (c) Stephan, D. W. *J. Am. Chem. Soc.* **2015**, *137*, 10018–10032. (d) Stephan, D. W. *Acc. Chem. Res.* **2015**, *48*, 306–316. (e) Stephan, D. W. *Science* **2016**, *354*, aaf7229.

(17) See for a comparison: (a) Mömning, C. M.; Otten, E.; Kehr, G.; Fröhlich, R.; Grimme, S.; Stephan, D. W.; Erker, G. *Angew. Chem., Int. Ed.* **2009**, *48*, 6643–6646. For some selected examples, see: (b) Peuser, I.; Neu, R. C.; Zhao, X.; Ulrich, M.; Schirmer, B.; Tannert, J. A.; Kehr, G.; Fröhlich, R.; Grimme, S.; Erker, G.; Stephan, D. W. *Chem. - Eur. J.* **2011**, *17*, 9640–9650. (c) Neu, R. C.; Ménard, G.; Stephan, D. W. *Dalton Trans.* **2012**, *41*, 9016–9018. (d) Ménard, G.; Gilbert, T. M.; Hatnean, J. A.; Kraft, A.; Krossing, I.; Stephan, D. W. *Organometallics* **2013**, *32*, 4416–4422. (e) Courtemanche, M.-A.; Larouche, J.; Légaré, M.-A.; Bi, W.; Maron, L.; Fontaine, F.-G. *Organometallics* **2013**, *32*, 6804–6811. (f) Stephan, D. W.; Erker, G. *Chem. Sci.* **2014**, *5*, 2625–2641.

(18) For a review, see: (a) Brintzinger, H. H.; Fischer, D.; Mülhaupt, R.; Rieger, B.; Waymouth, R. M. *Angew. Chem., Int. Ed. Engl.* **1995**, *34*, 1143–1170. For selected examples, see: (b) Jordan, R. F.; Dasher, W. E.; Echols, S. F. *J. Am. Chem. Soc.* **1986**, *108*, 1718–1719. (c) Chien, J. C. W.; Tsai, W. M.; Rausch, M. D. *J. Am. Chem. Soc.* **1991**, *113*, 8570–8571. (d) Bochmann, M.; Lancaster, S. J. *J. Organomet. Chem.* **1992**, *434*, C1–C5.

(19) (a) Parks, D. J.; von H. Spence, R. E.; Piers, W. E. *Angew. Chem., Int. Ed. Engl.* **1995**, *34*, 809–811. (b) Parks, D. J.; Piers, W. E.; Yap, G. P. A. *Organometallics* **1998**, *17*, 5492–5503.

(20) For a review, see: (a) Chen, E. Y.-X.; Marks, T. J. *Chem. Rev.* **2000**, *100*, 1391–1434. For examples, see: (b) Yang, X.; Stern, C. L.; Marks, T. J. *J. Am. Chem. Soc.* **1991**, *113*, 3623–3625. (c) Yang, X.; Stern, C. L.; Marks, T. J. *J. Am. Chem. Soc.* **1994**, *116*, 10015–10031. (d) Bochmann, M.; Lancaster, S. J. *Organometallics* **1994**, *13*, 2235–2243. (e) Deck, P. A.; Marks, T. J. *J. Am. Chem. Soc.* **1995**, *117*, 6128–6129.

(21) (a) Lauher, J. W.; Hoffmann, R. *J. Am. Chem. Soc.* **1976**, *98*, 1729–1742. (b) Tatsumi, K.; Nakamura, A.; Hofmann, P.; Stauffert, P.; Hoffmann, R. *J. Am. Chem. Soc.* **1985**, *107*, 4440–4451. (c) Hofmann, P.; Stauffert, P.; Tatsumi, K.; Nakamura, A.; Hoffmann, R. *Organometallics* **1985**, *4*, 404–406.

(22) See also: (a) Petersen, J. L.; Dahl, L. F. *J. Am. Chem. Soc.* **1975**, *97*, 6422–6433. (b) Erker, G.; Rosenfeldt, F. *Angew. Chem., Int. Ed. Engl.* **1978**, *17*, 605–606. (c) Erker, G.; Rosenfeldt, F. *J. Organomet. Chem.* **1980**, *188*, C1–C4. (d) Erker, G. *Acc. Chem. Res.* **1984**, *17*, 103–109.

(23) (a) Malone, J.; Parry, R. W. *Inorg. Chem.* **1967**, *6*, 176–177. (b) Malone, L. J.; Parry, R. W. *Inorg. Chem.* **1967**, *6*, 817–822.

(c) Spielvogel, B. F.; McPhail, A. T.; Knight, J. A.; Moreland, C. G.; Gatchell, C. L.; Morse, K. W. *Polyhedron* **1983**, *2*, 1345–1352. (d) Sood, A.; Spielvogel, B. F. *Inorg. Chem.* **1992**, *31*, 2654–2655. (e) Hall, I. H.; Rajendran, K. G.; Chen, S. Y.; Nordwood, V. N., III; Morse, K. W.; Sood, A.; Spielvogel, B. F. *Appl. Organomet. Chem.* **1994**, *8*, 473–480. (f) Alberto, R.; Ortner, K.; Wheatley, N.; Schibli, R.; Schubiger, A. P. *J. Am. Chem. Soc.* **2001**, *123*, 3135–3136.

(24) (a) Dobrovetsky, R.; Stephan, D. W. *J. Am. Chem. Soc.* **2013**, *135*, 4974–4977. (b) Berkefeld, A.; Piers, W. E.; Parvez, M.; Castro, L.; Maron, L.; Eisenstein, O. *J. Am. Chem. Soc.* **2012**, *134*, 10843–10851.

(25) (a) Sajid, M.; Kehr, G.; Daniliuc, C. G.; Erker, G. *Angew. Chem., Int. Ed.* **2014**, *53*, 1118–1121. (b) Elmer, L.-M.; Kehr, G.; Daniliuc, C. G.; Siedow, M.; Eckert, H.; Tesch, M.; Studer, A.; Williams, K.; Warren, T. H.; Erker, G. *Chem. - Eur. J.* **2017**, *23*, 6056–6068.

(26) Jian, Z.; Kehr, G.; Daniliuc, C. G.; Wibbeling, B.; Wiegand, T.; Siedow, M.; Eckert, H.; Bursch, M.; Grimme, S.; Erker, G. *J. Am. Chem. Soc.* **2017**, *139*, 6474–6483.

(27) Sajid, M.; Elmer, L.-M.; Rosorius, C.; Daniliuc, C. G.; Grimme, S.; Kehr, G.; Erker, G. *Angew. Chem., Int. Ed.* **2013**, *52*, 2243–2246.

(28) See also: (a) Burg, A. G.; Schlesinger, H. I. *J. Am. Chem. Soc.* **1937**, *59*, 780–787. (b) Fehlner, T. P.; Koski, W. S. *J. Am. Chem. Soc.* **1965**, *87*, 409–413. (c) Carter, J. C.; Moyé, A. L.; Luther, G. W., III. *J. Am. Chem. Soc.* **1974**, *96*, 3071–3073. (d) Umeyama, H.; Morokuma, K. *J. Am. Chem. Soc.* **1976**, *98*, 7208–7220. (e) Goldman, A. S.; Krogh-Jespersen, K. *J. Am. Chem. Soc.* **1996**, *118*, 12159–12166. (f) Fukazawa, A.; Dutton, J. L.; Fan, C.; Mercier, L. G.; Houghton, A. Y.; Wu, Q.; Piers, W. E.; Parvez, M. *Chem. Sci.* **2012**, *3*, 1814–1818.

(29) For selected examples, see: (a) Dureen, M. A.; Stephan, D. W. *J. Am. Chem. Soc.* **2009**, *131*, 8396–8397. (b) Jiang, C.; Blacque, O.; Berke, H. *Organometallics* **2010**, *29*, 125–133. (c) Dureen, M. A.; Brown, C. C.; Stephan, D. W. *Organometallics* **2010**, *29*, 6594–6607. (d) Wang, X.; Kehr, G.; Daniliuc, C. G.; Erker, G. *J. Am. Chem. Soc.* **2014**, *136*, 3293–3303.